International Symposium
Non-Destructive Testing in Civil Engineering (NDT-CE)

September 15 - 17, 2015, Berlin, Germany

Elastic wave propagation of ultrasound in bituminous road surfaces – simulations and measurements

Stefan MAACK[1], Guido KNEIB[2]

[1]BAM, Federal Institute for Materials Research and Testing, Unter den Eichen 87, 12205 Berlin, Germany, Phone +493081044246, Fax: +493081041447; e-mail: stefan.maack@bam.de

[2]Müller-BBM Schweiz AG, Gewerbestrasse 25, 4123 Allschwil, Switzerland, Phone +41616902603, Fax: +41616902609; e-mail: guido.kneib@mbbm.com

Abstract

Maintenance costs of road infrastructure are increasing steadily. The main cause of this is the nearly exponential increase of traffic during the last decades. Adverse environmental impacts on infrastructure get more and more important as well. Therefore, it is important to determine how limited financial resources can be directed with an optimum pay-out. Often a decision has to be made whether existing structures have to be rebuilt or repaired based on the condition of the structures.

The present study takes first steps towards the usage of low-frequency ultrasound as a tool to evaluate the road condition. The overall aim is to derive a prediction model for future road conditions. In order to better understand and interpret recorded wave fields simulations of elastic wave propagation in layered and scattering road models have been performed. The study combined investigations in the laboratory with field measurements.

In a series of extensive laboratory tests with different asphalt mixtures characteristic wave properties have been derived. Travel time (resp. velocity) as important material parameter has been investigated for different wave types, different centre frequencies and at various temperatures. An investigation of the directivity of wave radiation in the heterogeneous asphalt bodies led to an estimate of the related disturbing influences.

Based on the laboratory results field measurements were performed on a real road and the records were processed to identify layers, propagation speeds and attenuation. The results were verified by a series of simulations.

Keywords: bituminous material, road inspection, elastic waves, ultrasound, non-destructive testing

1. Introduction

The classification of road condition in Germany is based on different criteria. Among them are the grip of the road surface, its evenness or the number and size of visible cracks. These criteria are quantified following an assessment scheme that yields a condition number. The planning and performing of maintenance measures are based on this condition number. In order to control and to maintain the performance of road infrastructure in line with the increasing demand, reliable and informative evaluation methods are required that allow the quantification of the inner road condition.

The mechanical properties of a road body indicate its inner condition. Currently destructive methods, like core extractions are in use. In order to avoid damage by the evaluation procedure the non-destructive Falling Weight Deflector (FWD) method is applied and the results are extrapolated on the traffic network. The FWD method is time-consuming and it characterizes only the complete road body consisting of bounded and unbounded layers. A separate evaluation of the different road layers is not possible although the classification of the bounded layers is of particular interest.

This research work aims at the possibilities to determine material properties via elastic waves at low ultrasonic frequencies. The results presented here are based on a research project sponsored by the German Federal Road Research Institute [1]. The task was to investigate in how far commercially available measuring techniques can achieve this with an effort that is acceptable in practice. The method of reflection seismology as originating from geophysics is adopted and applied. In reflection seismology source and receiver points are placed along

lines or in areal patterns on a measuring surface such that single measurements can be combined and displayed as time-space curves.

Investigations in the laboratory yield material properties that can be used for wave field simulations in a layered road body. Material parameters are determined as a function of temperature. On a real road (federal road B35 near Illingen) measurements were taken, processed and interpreted. The layering at the test site is well documented [2].

2. Laboratory investigations to characterize the material

Simulations of elastic wave propagation require elastic material models of the velocities of longitudinal and transversal waves and of the density. The time-space histories of wave fields are simulated comprising different wave types and wave modes. Since wave velocities are linked to other elastic material parameters they can be understood as a proxy for the mechanical condition of the medium.

A literature search has concluded that sound velocities in bituminous material vary strongly. Apart from differences in material composition the temperature dependence of the material is most important. In a first step the propagation times of four asphalt specimen with different compositions were determined. The mixtures correspond to the material at the test site. The specimens were cut at equidistant intervals of 340 mm such that the probes could be measured at three different lengths (340 mm, 260 mm, 180 mm) to compare travel times and amplitudes. The temperature in a climatic chamber has been increased from 0° C in steps of 5° C up to 50 °C.

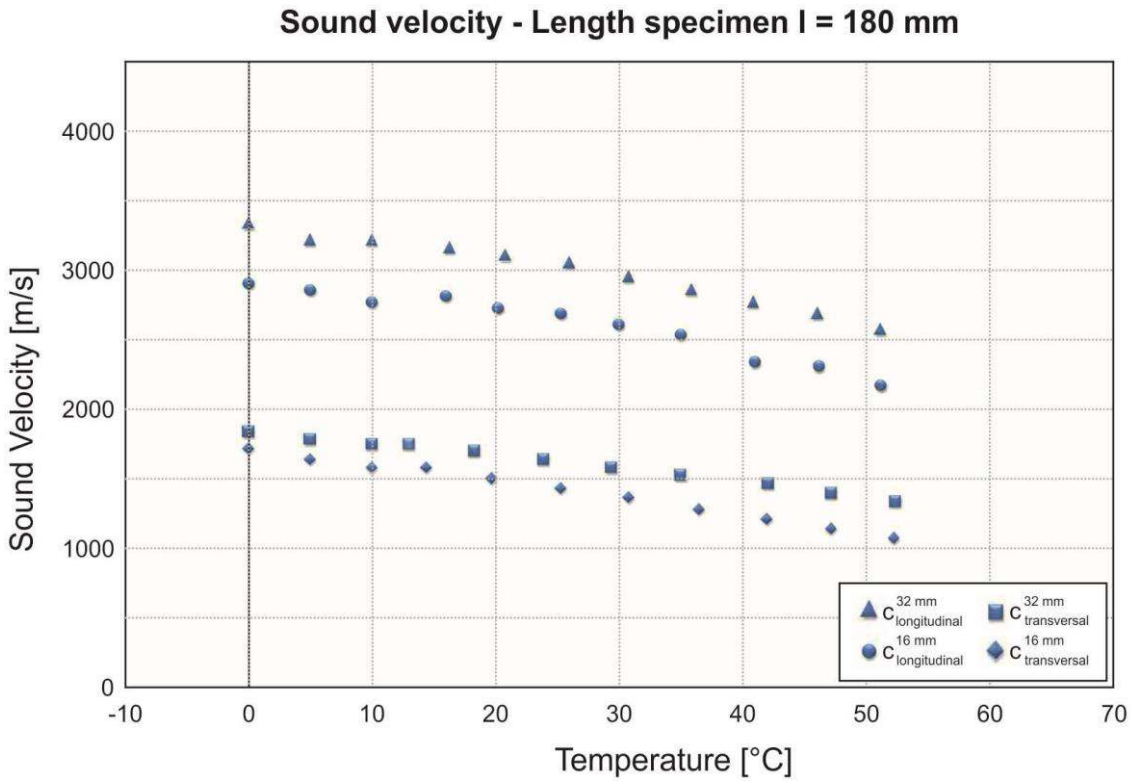

Figure 1: Diagram of the sound speed of the different wave types of the specimen with a length of 180 mm. The middle frequency for the longitudinal wave is 100 kHz and for the transversal wave 50 kHz.

Figure 1 shows temperature-dependent velocities of longitudinal and transversal waves. The longitudinal wave had a center frequency of 100 kHz and the transversal wave of 50 kHz. The

decrease of wave speed with temperature is obvious. Also note that larger travel times were observed in mixtures with larger grain sizes.

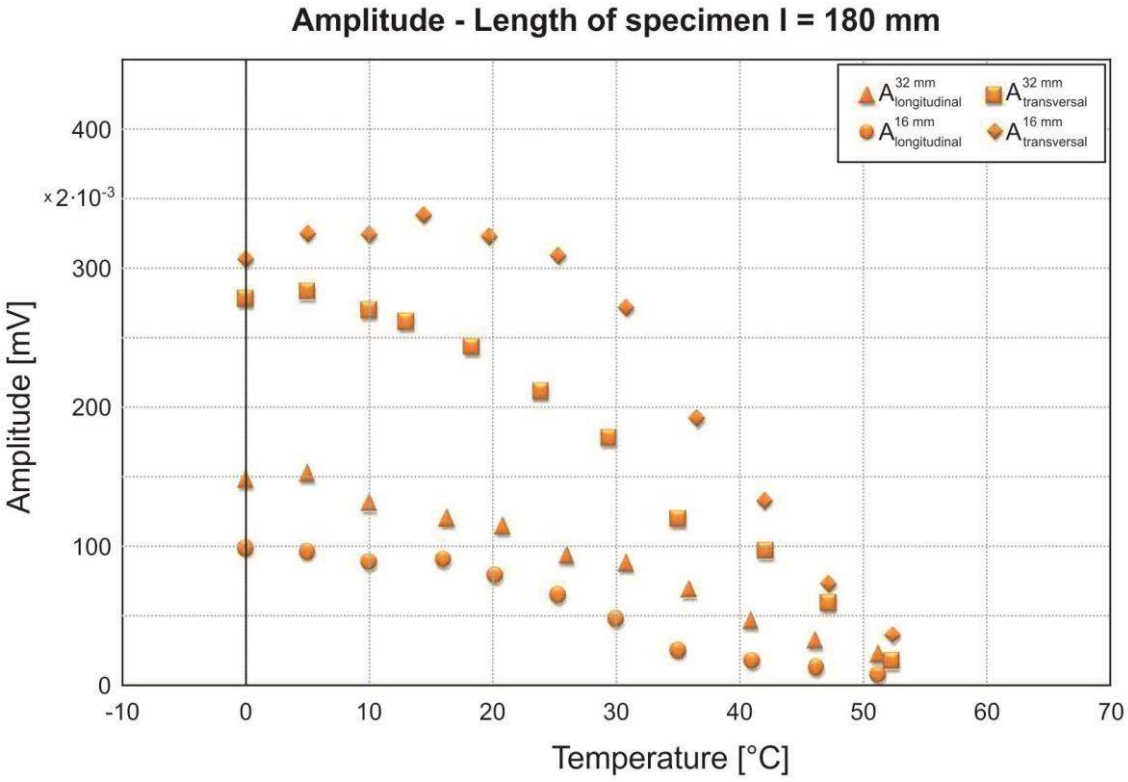

Figure 2: Amplitudes of different wave types in relation to the material temperature measured on specimens with lengths of 180 mm

Figure 2 displays signal strength as function of temperature. Note that relative amplitudes are shown such that amplitudes of longitudinal and transversal waves cannot be compared directly. As expected amplitudes of all wave types decrease quickly with temperature. At temperatures above 50 °C signals became so weak that they were difficult to be detected.

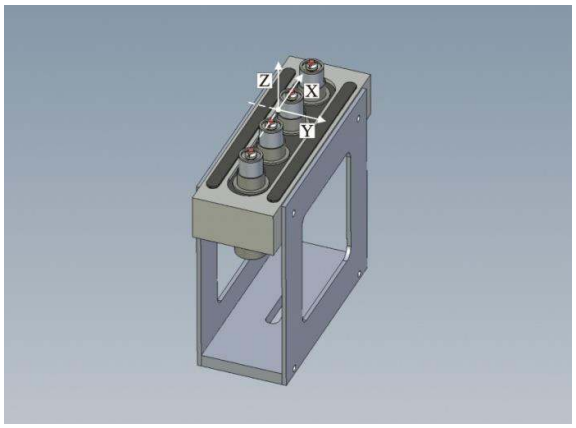

Figure 3: Ultrasonic array used for measurements comprised of 4 single commercially available probes [3]

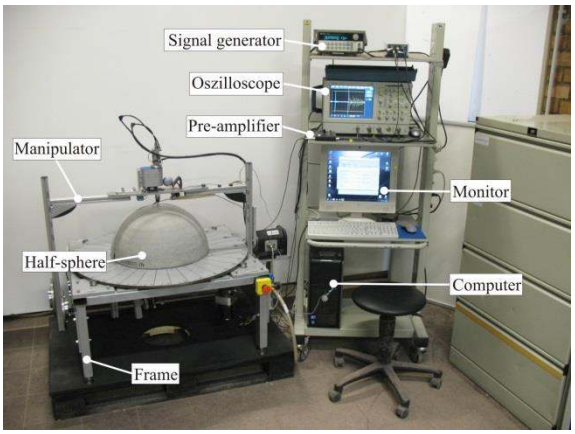

Figure 4: Automatic scanning system built at BAM with scanner and half sphere specimen (left) and data processing unit (right) [4]

Besides the material parameters the geometry of the wave field radiation is important. For the related investigations commercial probes were used that have been modified in their geometrical layout by the BAM (Figure 3). The source wave front is created when all probes

vibrate in parallel. The superposition of the pulses approximates a point source in the plane parallel to y while the layout with four probes in line allows emission of more energy into the specimen. The determination of the spatial wave field is performed via an automatic scanner developed at the BAM (Figure 4). Measurements were taken at a polyamide reference specimen as well as at various asphalt specimens.

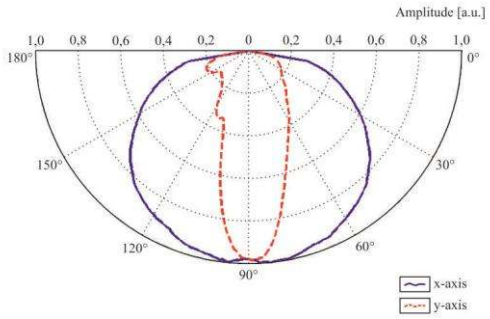

Figure 5: Directivity pattern for longitudinal excitation on polyamide for the probe in Figure **3** [3]

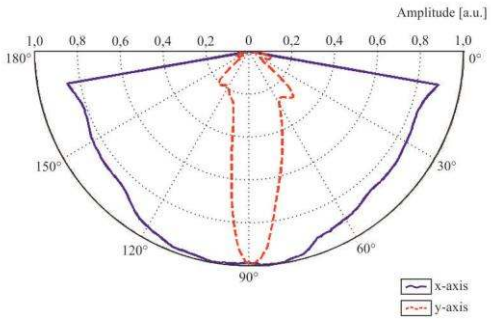

Figure 6: Directivity pattern for transversal excitation on polyamide for the probe in Figure **3** [3]

Figure 5 and Figure 6 display the directivity patterns of the used probes (shown in Figure 3) at the reference body of polyamide. Shown are results for the x-z-planes (red) and the y-z-planes (blue). The directivity in the x-z-plane approximates that of a point source [5, 6].

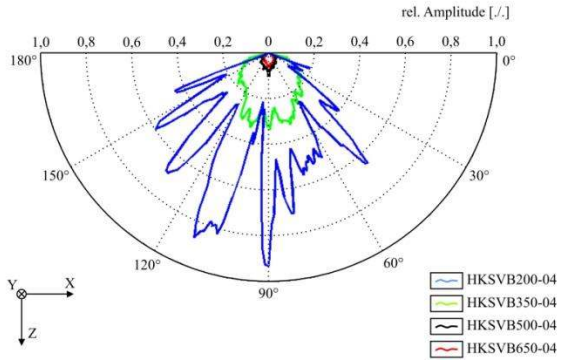

Figure 7: Directivity pattern for longitudinal excitation on bituminous specimens with different radii (200 mm, 350 mm, 500 mm, 650 mm; maximum aggregate diameter 16 mm) [3]

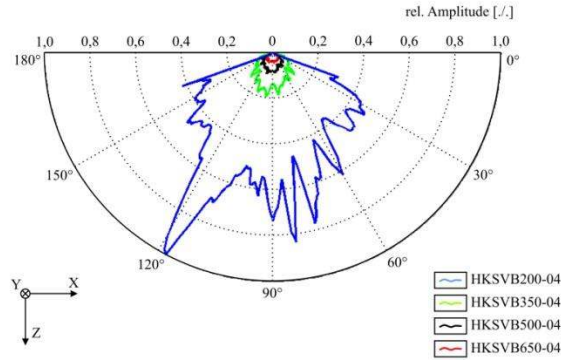

Figure 8: Directivity pattern for transversal excitation on bituminous specimens with different radii (200 mm, 350 mm, 500 mm, 650 mm; maximum aggregate diameter 16 mm) [3]

Figure 7 and Figure 8 show polar diagrams of directivity patterns for used probes on different specimens. In Figure 7 the results for the longitudinal wave probe are displayed in the y-z-plane. Figure 8 shows directivity patterns for the transversal probe in the y-z-plane. The high variations in the amplitudes are due to the rough surface of the specimens and the local grain distribution. As a result a qualitative correspondence with the reference measurements on polyamide can be ascertained.

3. Measurements on federal route B35 at Illingen

Within the framework of the research project the results from the laboratory had to be verified in a field test on a real road. This asked for a detailed and reliable documentation of the selected road body which was available at a section of the federal road B35 near Illingen where previous research projects to evaluate road condition had taken place [2]. The section profile is sketched in Figure 9 together with the measurement geometry.

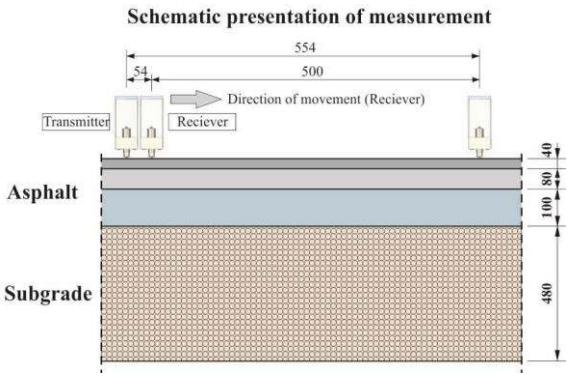

Figure 9: Schematic presentation of road structure with different layers and of the measurement positions of source and receivers.

Figure 10: Measurement on highway B35 near Illingen (Germany) with the automatic scanner system [1]

Measurements were performed with an automatic scanner system (Figure 10). The scanner had been programmed to allow for 250 receiver positions at intervals of 2 mm (Figure 9) while the transmitter has remained stationary. Source-receiver offsets covered a range from 54 mm to 554 mm. Data has been acquired with the probe vibrating in transversal as well as in longitudinal direction. Longitudinal excitations had a center frequency of 100 kHz and the transversal excitations of 50 kHz.

4. Data analysis and comparative simulations

In this publication only selected results from the field test can be presented. More information can be found in the final research report [1].

The transversal vibrations of the probe transmit a horizontally polarized shear wave into the half space (SH-wave) which results in a direct S-wave with particle motions parallel to the x-axis (see also Figure 3). In contrast longitudinal vibrations of the probe lead to a vertically polarized surface wave and a compressional wave moving downward (P-SV-case). The compressional and shear vibrations in vertical directions are coupled. In granular media with rough surfaces such as asphalt all wave types with suitable wavelengths are converted at the grain boundaries resulting in a very complex wave field. For example direct longitudinal waves are recordable in case of transversal source vibrations at the surface and also different kinds of scattered waves.

In order to better understand the recorded wave fields and to interpret the observed events it is very useful to perform simulations of wave propagation. In this work an algorithm that solves the elastodynamic equations of motion via a finite-difference algorithm is used [7]. In a series of simulations we applied source wavelets similar to the pulses emitted by the probes in the field measurements and elastic models of varying degrees of complexity. A simple three layer model comprised a 220 mm asphalt body, an antifreezing layer of 480 mm and a sandy

ground layer below of 55 mm. The respective model velocities were based on the laboratory measurements and a first analysis of the field data. For example the slope of time-offset curves of the direct shear wave corresponds to the inverse of the shear wave velocity. In another model variation the homogeneous layers were replaced by granular layers where the grain sizes vary according to the grain distribution used in the mixtures for the test site.

Figure 11 presents a snapshot of a simulation through the granular 2-D model, 200 µs after the initiation of the point force at the surface. Shown are the horizontal x-component (upper left), the vertical z-component (upper right), the shear component (lower left) and the pressure component (lower right). Figure 12 displays snapshots of wave propagation after 200 µs, 400 µs, 600 µs and 800 µs for isotropic homogeneous layers. In studying the snapshots and the corresponding synthetic time-space records it is possible to interpret the measurement results in detail and to annotate certain events as in Figure 13, right. There, the recorded wave fields are shown after processing. The processing aims to enhance wave events of interest and to suppress unwanted signal via digital signal processing. Without going into detail here, key methods applied were filtering based on a singular value decomposition of the data matrix [8] and the radon transform.

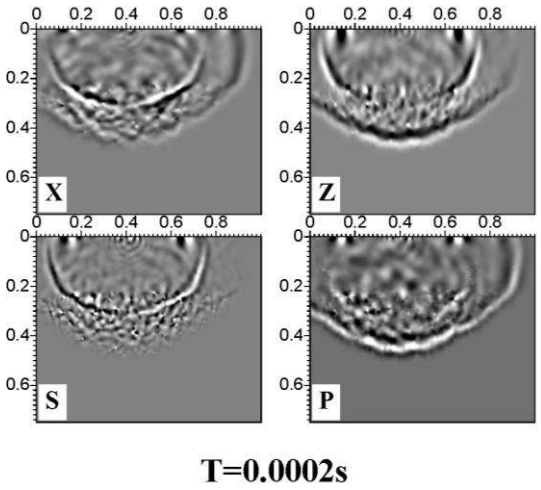

Figure 11: Snapshot of the simulation in the granular 2-D model after 200 µs. Shown are the horizontal x-component (upper left), the vertical z-component (upper right), the shear component (lower left) and the pressure component (lower right).

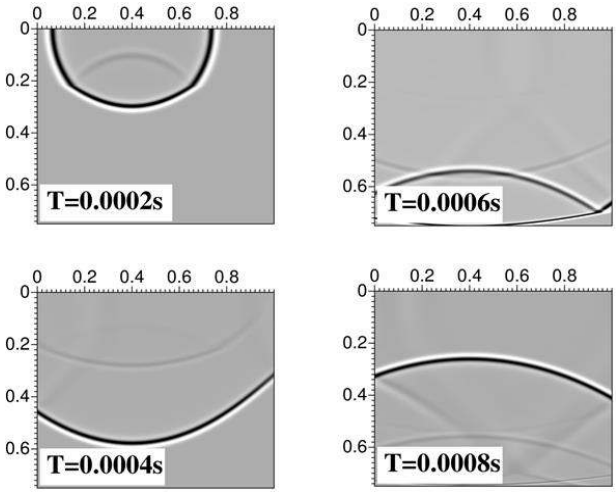

Figure 12: Snapshots of wave propagation after 200 µs, 400 µs, 600 µs and 800 µs for a model with three homogeneous layers.

The following Figure 13 shows filtered raw data from the field test after transversal excitation of the probes (left), the corresponding simulation result (center) and the final processed shot record (right). Note that the simulation is based on a simplified model with a homogeneous asphalt body. The Reflection form the base of the asphalt can already be seen in the filtered raw data. A direct longitudinal wave as visible in the filtered data cannot exist in a homogeneous asphalt layer in case of SH sources and therefore is missing in the simulation. The raw data also displays reflections from surface heterogeneities which are dipping from upper right to lower left (see arrow). The processed data shows reflections from the three layer boundaries and many scattered waves.

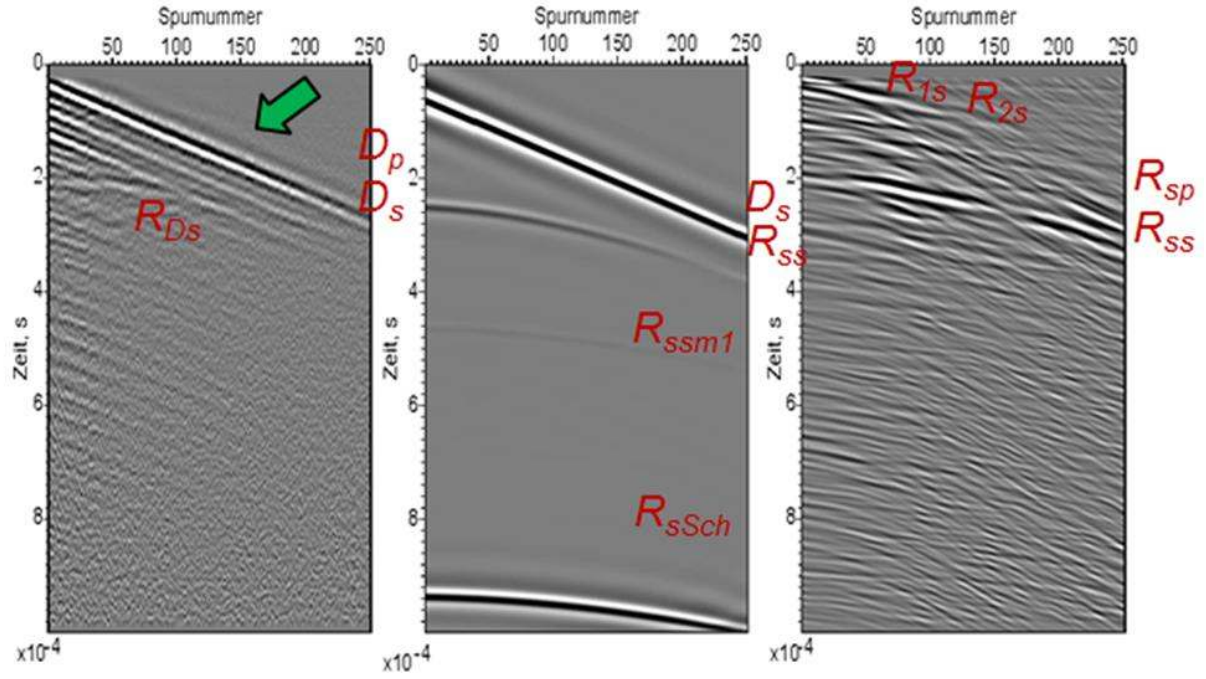

Figure 13: Filtered raw data from the field test after transversal excitation of the probes (left), the corresponding simulation result (center) and the final processed shot record (right).

In Figure 13 some events are annotated and the corresponding abbreviations are listed in Table 1. The case of longitudinal source vibrations is shown in Figure 14: Filtered raw data from the field test after longitudinal excitation of the probes (left), the corresponding simulation result (center) and the final processed shot record (right). Figure 14. Converted wave reflections from the lower boundary of the asphalt can be seen well in the simulation and in the processed data. Most remarkable is the observation of the reflection from the lower boundary of the anti-freezing layer in a known depth of 700 mm.

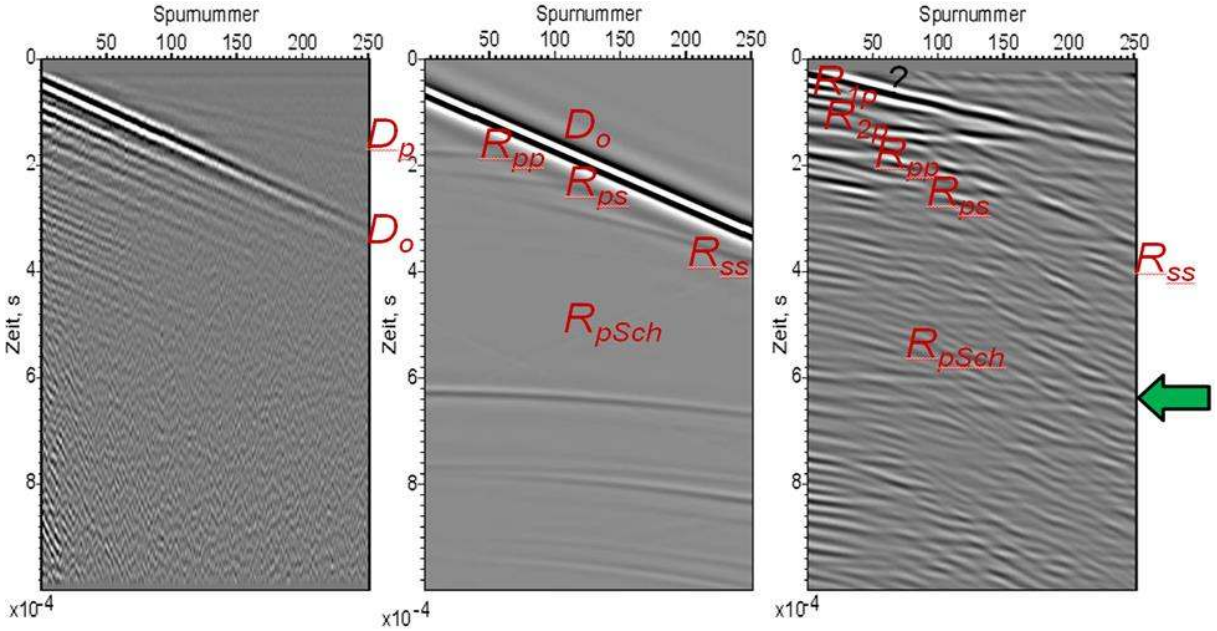

Figure 14: Filtered raw data from the field test after longitudinal excitation of the probes (left), the corresponding simulation result (center) and the final processed shot record (right).

Table 1: Corresponding abbreviations in Figure 13 and Figure 14

Abbreviation	Description
D_p	direct P-wave
D_s	direct S-wave
D_O	direct surface wave
R_{Ds}	S-wave reflection at surface heterogeneities
R_{1s}	S-wave reflection from lower boundary of asphalt cover
R_{2s}	S-wave reflection from lower boundary of binder layer
R_{sp}	S-P reflection from lower boundary of asphalt layer
R_{ss}	S-S reflection from lower boundary of asphalt layer
R_{ssm1}	First multiple S-reflection from anti-freezing layer
R_{sSch}	S-reflection from anti-freezing layer
R_{pp}	P-P reflection from lower boundary of asphalt layer
R_{ps}	P-S reflection from lower boundary of asphalt layer
R_{pSch}	P reflection from anti-freezing layer
R_{1p}	P reflection from lower boundary of asphalt surface layer
R_{2p}	P reflection from lower boundary of binder layer

The results from the field measurements that are not shown here led to corresponding shot gathers [1].

5. Conclusions and Outlook

The research project has shown that the layering of road bodies can be identified via ultra sound. Laboratory measurements at selected asphalt specimen left their mark in synthetic models for wave field simulations. Laboratory measurements, field tests and simulations yielded new insights and practical experiences that should be taken further. The investigations in the laboratory showed a velocity decrease about 30 percent when the asphalt temperature increased from 0 °C to 50 °C. This corresponds to ultrasonic investigations in tar sands but is in contrast to published values from roads at much lower frequencies of few Hertz, like for example measurements via Falling Weight Deflectometer. At the low FWD frequencies a much larger temperature dependence of several hundred percent is observed in the temperature range of interest which favours ultrasonic investigations.

References

1. Kneib, G., Maack, S., Forschungsbericht: Innovative zerstörungsfreie Untersuchungen des Schichtaufbaus von Straßen, Bundesanstalt für Straßenwesen (BASt), FE04.0267/2012/BRB (in print, german)

2. Wellner, F., Oeser, M., Weise, C., Jähnig, J., Leutner, R., Lorenzl, H., Schindler, K., Mollenhauer, K., 2007, Nachhaltiger Straßenbau –Bemessungsmodell zur Förderung der Innovations- und Wettbewerbsfähigkeit kleiner und mittelständischer Straßenbauunternehmen, Schlussbericht zum Projekt FKZ 19W3055E (german)

3. Müller, S., Thema: Weiterentwicklung der Reverse Time Migration zur Anwendung auf Ultraschall-Echo-Daten in der zerstörungsfreien Prüfung, Doktorarbeit, Freie Universität Berlin, in Veröffentlichung (vorrausichtlich 2015).

4. Spies, M.; Rieder, H.; Orth, T.; Maack, S.: Simulation of ultrasonic arrays for industrial and civil engineering applications including validation. REVIEW OF PROGRESS IN QUANTITATIVE NONDESTRUCTIVE EVALUATION: Volume 31. AIP, 2012, S. 841–848.

5. Miller, G. F.; Pursey, H.: The Field and Radiation Impedance of Mechanical Radiators on the Free Surface of a Semi-Infinite Isotropic Solid. Proceedings of the Royal Society A: Mathematical, Physical and Engineering Sciences 223 (1954), 1155, S. 521–541.

6. Langenberg, K. J., Märklein, R., Mayer, K.: Ultrasonic Nondestructive Testing of Materials – Theoretical Foundations. Taylor & Francis ISBN 978-1-4398-5588-1, 2012

7. Kneib, G., Leykam, A.: Finite-difference modeling for tunnel seismology, Near Surface Geophysics, 2, 71-93, 2004.

8. Kneib, G., Bardan, V.: 3D targeted multiple attenuation, Geoph. Prosp., 45, 701-714., 1997.